Yordkayhun, S., Ivanova, A., Giese, R., Juhlin, C., Cosma, C. (2009): Comparison of surface seismic sources at the CO2SINK site, Ketzin, Germany. - Geophysical Prospecting, 57, 1, 125-139

DOI: 10.1111/j.1365-2478.2008.00737.x

Comparison of surface seismic sources at the CO_2SINK site, Ketzin, Germany

Sawasdee Yordkayhun[1*], Alexandra Ivanova[2], Ruediger Giese[2], Christopher Juhlin[1], and Calin Cosma[3]

[1]*Department of Earth Sciences/Geophysics, Uppsala University, Uppsala, Sweden,*
[2]*GeoForschungsZentrum, Section 5.1, Potsdam, Germany,*
[3]*Vibrometric, Vantaa, Finland*
(E-mail: sawasdee.yordkayun@geo.uu.se / Fax: +46 18-501110 / Phone: +46 18-471 7161)

Geophysical Prospecting, in press.

ABSTRACT

In 2004 three seismic surface sources (VIBSIST, accelerated weight drop and MiniVib) were tested in a pilot study at the Ketzin test site, Germany, a study site for geological storage of CO_2 (EU project CO_2SINK). The main objectives of this pilot study were to (1) evaluate the response of the Ketzin site to reflection seismics, especially at the planned injection depth, (2) test different acquisition parameters and (3) use the results to guide the planning of the 3D survey. As part of these objectives, we emphasize the source performance comparison in this study. The sources were tested along two perpendicular lines of 2.4 km length each. Data were acquired by shooting at all stations (source and receiver spacing of 20 m) on both lines, allowing CMP stacked sections to be produced. Sources signal characteristics based on signal-to-noise ratio, signal penetration and frequency content of raw shot records were analyzed and stacked sections were compared. The results show that all three surface sources are suitable for reflection seismic studies down to a depth of about 1 km and provide enough bandwidth for resolving the geological targets at the site, i.e., the Weser and Stuttgart Formations. Near surface conditions, especially a thick weathering layer present in this particular area, strongly influence the data quality, as indicated by the difference in reflectivity and signal-to-noise ratio of the two CMP lines. The stacked sections of the MiniVib source show the highest frequency signals down to about 500 ms traveltime (approx. 500 m depth), but also the shallowest signal penetration depth. The VIBSIST source generates signals with the highest signal-to-noise ratio and greatest signal penetration depth of the tested sources. In particular, reflections below 900 ms (approx. 1 km depth) are best imaged by the VIBSIST source. The weight drop performance lies in between these

two sources and might be recommended as an appropriate source for a 3D survey at this site because of the shorter production time compared to the VIBSIST and MiniVib sources.

INTRODUCTION

Geological storage of CO_2 may contribute significantly to reduce CO_2 emissions into the atmosphere in the near future (Metz *et al.* 2005). Tracking the CO_2 after it is injected into the underground reservoir and detecting any leakage out of the reservoir is an important component of large scale storage. The CO_2SINK project (Förster *et al*. 2006), funded in part by the European Commission, focuses on the application of various monitoring techniques for geological storage of CO_2. It includes both theoretical and applied scientific studies related to the characterization of the sub-surface and to understanding the processes associated with the storage of CO_2. The main objectives are to (1) investigate and advance the understanding of the science and practical processes related to geological storage of CO_2 in a saline aquifer, (2) build confidence towards future European geological storage of CO_2 and (3) provide real case experience that can be used in the development of future regulatory frameworks for geological storage of CO_2.

In order to attain the above objectives a study site located west of Berlin, near the city of Ketzin, Germany (Figure 1) has been selected. The Ketzin site served as a natural gas storage facility from the 1970s until 2000. The existing infra-structure from the natural gas storage facility was an important consideration in choosing the site. Even though the CO_2SINK project involves only injection of CO_2 on a small scale (30,000 tons/year) the methodology to be employed is similar to what will be used on a larger scale. Prior to drilling the injection borehole, a pre-investigation phase was performed consisting of compilation of available geological information, modeling studies, and evaluation of geophysical and geochemical techniques. An important component in this pre-drilling phase was a 3D baseline seismic survey (Juhlin *et al*. 2007). In 2007, three boreholes, one injection well and two monitoring wells, about 50–100 m apart, were drilled into the flank of the Ketzin anticline. Starting in 2008, approximately 100 tons/day of nearly pure CO_2 will be injected at about 650 m depth into a saline sandstone aquifer and continuing for up to 2 years. During and after injection, extensive monitoring of the distribution of the injected CO_2 will be carried out by using a broad range of geophysical and geochemical techniques, as well as reservoir modeling.

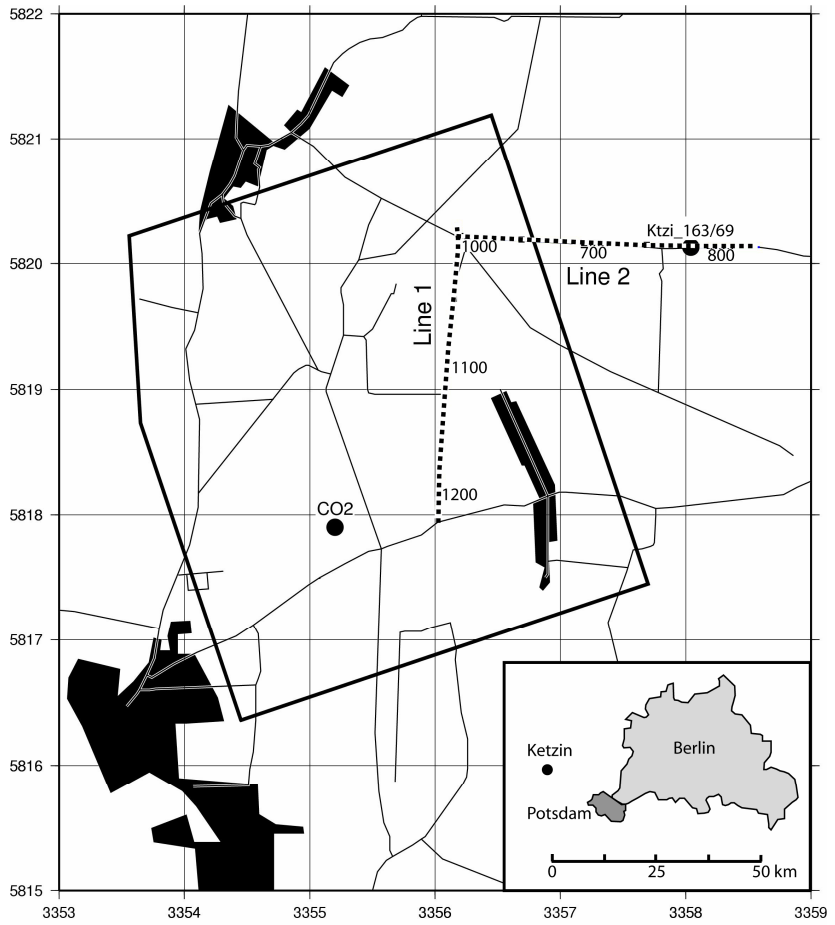

Figure 1. Map of the Ketzin pilot study area close to Potsdam, Germany. The two CDP profiles are marked as Line 1 (N-S profile) and Line 2 (E-W profile). Borehole Ktzi 163/69 is indicated by the black circle. The area marked by the polygon approximately encloses the area for the main 3D survey. The expected injection site is also indicated (Black circle marked as CO2).

Studies elsewhere (Davis *et al*. 2002, Arts *et al*. 2004, Ziqiu and Takashi 2004) have shown that seismic methods perform well in tracking the movement of CO_2 in the sub-surface using time-lapse techniques. Before carrying out the 3D baseline seismic survey at the Ketzin site, a pilot study was performed in 2004 (Figure 1). The main objectives of this pilot study were to (1) evaluate the response of the Ketzin site to reflection seismics, especially at the planned injection depth, (2) test different acquisition parameters, such as surface seismic sources, geophone types and their deployment, and recording parameters, and (3) use the results to guide the planning of the 3D survey. Vintage seismic data from the 1960s showed that it was possible to obtain good seismic images using several kilograms of dynamite as a source.

However, use of dynamite has become difficult due to permitting and cost. Since the 3D seismic survey would require a large number of source points, the time necessary to activate a source was an important factor to consider, as well as the source performance with respect to penetration depth and frequency content. Therefore, in this paper we focus on the comparison of the three seismic sources used in the pilot study: VIBSIST, MiniVib and weight drop. We compare penetration depth and frequency content using individual source gathers, followed by comparisons of stacked sections along two different test lines. Finally, we discuss the advantages and disadvantages of the three different sources.

SITE GEOLOGY

Vintage reflection seismic profiles, stratigraphic, and lithological information obtained from the many shallow boreholes drilled in the area provide information about the sub-surface geology of the studied area. The Ketzin site is located on the eastern part of a salt generated double anticline structure, the Roskow-Ketzin anticline (Figure 2), with an axis striking NNE-SSW and flanks gently dipping at about 15°. The topography of the Ketzin site is relatively flat, but does contain some isolated highs, consisting mainly of Quaternary sands. This unit hosts the main freshwater aquifer in the area. Below the Quaternary deposits, Tertiary, Lower Jurassic and Triassic rocks are present, consisting mainly of sandstones, siltstones and mudstones. A Tertiary clay (the Rupelton), about 80–90 m thick, forms the caprock for the underlying aquifer system. This Tertiary clay acts as a major aquitard separating the saline waters (brines) in the deeper aquifers from the non-saline groundwater in the shallow Quaternary aquifers. There is evidence that local erosion of the Rupelton aquitard at some locations (Förster *et al*. 2006) allows saline waters to ascend and mix with fresh water in the shallow aquifers. The Jurassic sandstones between 250 m and 400 m were used for the industrial storage of natural gas until the year 2000. These sandstones, together with inter-layered mudstone, siltstone, and anhydrite form a multi-aquifer system. Within the Triassic units, playa-type rocks of the Weser and Arnstadt Formations, consisting mainly of claystone, silty claystone, and the Keuper anhydrite, form an approximately 210 m thick caprock section above the Stuttgart Formation. The approximately 20 m thick anhydrite layer present within the caprock is known as the K2 (Keuper) reflector. This high impedance layer, found between depths of 500 m to 700 m at the Ketzin site, has been clearly imaged on the vintage seismic data and is an important marker horizon for the CO_2SINK project since it lies about 80 m above the top of the Stuttgart Formation, the target formation for the CO_2 injection at Ketzin. The Stuttgart Formation is on average 80 m thick and lithologically heterogeneous. Important horizons in this study are : 1) the T1 horizon, i.e. the transgression phase of the Cenozoic or Base Tertiary; 2) the assumed L4

horizon at the base of the Hettangian (near Top Triassic); 3) the K2 horizon, i.e. the top of the Heldburg-gypsum at the top of the Weser Formation; and 4) the K3 horizon, i.e. the top of the 'Oberer Hauptgips', a gypsum or anhydrite at the top of the Grabfeld Formation, close to the base of the Stuttgart Formation (Reinhardt 1993).

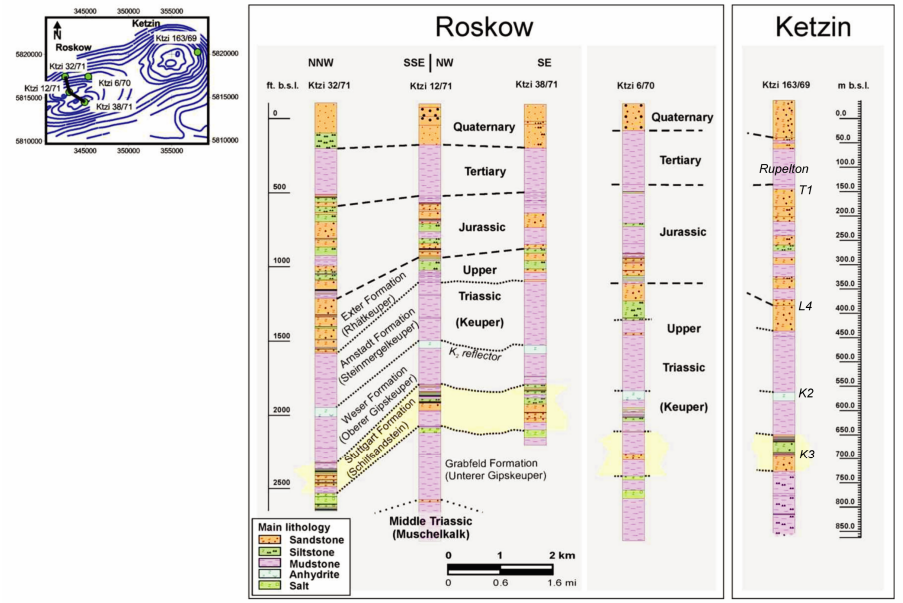

Figure 2. Geological structures of the site inferred from a local borehole (163/69) in Ketzin and adjacent boreholes. The main possible reflection horizons are marked (T1, L4, K2 and K3).

SEISMIC SOURCES

Choice of seismic sources

Explosives are high-energy and high-bandwidth seismic sources, but permitting and expensive drilling operations make these sources unsuitable in many cases. Alternatives, such as vibrators on land (e.g. Woodward 1994; Steer *et al.* 1996) and airguns at sea (e.g. Staples *et al.* 1999) have been used for reflection seismic profiling for hydrocarbon exploration and deep seismic profiling. For small-scale land surveys, a large number of land seismic sources have been developed and successfully applied to shallow engineering, groundwater, mining and environmental problems (e.g. Pullan and MacAulay 1987; Jongerius and Helbig 1988; Steeples and Miller 1990; Wright *et al*. 1994). The choice of the most suitable seismic source depends on the target and the required penetration depth and resolution. Vertical resolution is controlled by the frequency band of the source, whereas target depth

and acquisition parameters also influence the spatial resolution. Several studies have dealt with various aspects of sources, for example, site dependence and environmental conditions, energy and frequency content, signal-to-noise ratio, source wavelet, repeatability, portability and efficiency.

The energy and frequency content required from a seismic source to record seismic reflections depends on many factors, including the depth of the target and its thickness (Knapp and Steeples 1986). Selecting seismic sources capable of generating adequate broad bandwidth is important because seismic resolution depends on the dominant frequency of the signal. The energy of a seismic wave can be quantified by the energy density (energy per unit volume) which is proportional to the square of the amplitude within the same medium (Sheriff 1975; Telford *et al*. 1990). Amplitude is limited by both non-geological factors (e.g. source strength and coupling) and geological (sub-surface) factors. In particular, seismic attenuation increases exponentially with increasing frequency of the seismic signal and decreasing quality factor (Q) of the probed medium (Buhnemann and Holliger 1998).

Even if there are no substantial differences in frequency content, the source can significantly influence the signal-to-noise ratio (Feroci *et al*. 2000). Air blasts and source generated noise, especially noise due to the coupling effect of impact sources, can be so large in amplitude that they contaminate all the reflections on near offset traces. In areas where random noise dominates, vertical stacking improves the signal-to-noise ratio if the source is repeatable. However, if the noise is due to source coupling then vertical stacking will not lead to improvement.

For 3D surveys, a large number of shots are generally required; therefore, the cost, time, and portability are important factors that should not be neglected when choosing a seismic source.

Seismic sources in this study

Three seismic sources were tested in the pilot study at the CO_2SINK Ketzin site; an accelerated weight drop, a MiniVib (vibrator) and a VIBSIST source (Figure 3). The first two are well known within the seismic exploration community. The accelerated weight drop is an impact source (Figure 3a). Momentum at impact, size (mass) of the base plate, and near surface conditions influence the amplitude and frequency content of the signal. Since the signal pulse input energy of this source is relatively low and uncontrollable, significantly decreased signal-to-noise ratios result when the wave propagates at great distances. However, vertical stacking increases energy without lengthening the wavelet if the source unit has good repeatability. To ensure repeatability, the ground below the base plate should be compacted before production recording begins. The source is controlled by a trigger sensor (opto-coupler) mounted on the base plate which transmits the trigger pulse to the recording system by radio link. The trigger inaccuracy is less than 1 ms and variations greater than this were not noted in our survey.

a) Weight drop

b) MiniVib

c) VIBSIST

Figure 3. (a) Weight drop source. (b) MiniVib source. (c) VIBSIST source.

The MiniVib (Figure 3b) uses a swept frequency signal (sweep) that changes frequency at constant amplitude from a low limit f_1 to a high limit f_2 over a period of seconds. A linear sweep of 30-150 Hz was used for the data presented here. Since the used MiniVib is designed for relatively high resolution surveys, technical limitations do not allow frequencies below 30 Hz to be employed since resonances might occur and damage the system. The coupling of the vibrator to the ground introduces limitations for the high end of the sweep frequency. After acquisition, the field records were cross-correlated with a reference signal (the measured pilot sweep). The correlation process using the sweep yields, in theory, a zero phase wavelet. However, in practice the correlated signal is mixed phase due to sweep specifications, vibrator imperfections and ground coupling.

VIBSIST sources have just been developed over the past decade and are based on the Swept Impact Seismic Technique (Park *et al*. 1996), a combination of the Vibroseis swept-frequency and the Mini-Sosie (Barbier *et al*. 1976) multi-impact methods (Figure 3c). A few to several hundred impulsive seismic pulses are generated according to a preset monotonic impact sequence in which the impact rate either increases linearly with time (upsweep) or decreases with time (downsweep). In our survey an initial impact time spacing of about 1100 ms between impacts was used and it decreased linearly to about 200 ms between impacts at the end of the sweep. The impact sequence was controlled by a pilot trace recorded by a sensor (geophone) placed on the ground near the impact plate. The operation and the sweep function tuning of this source is done by using the VIBSIST controller interface. The decoding process is a "shift-and-stack" method that is simpler and quicker than cross-correlation. In our "shift-and-stack" method all recorded impacts are combined into a single file prior to processing. Therefore, no direct vertical stacking of shots is performed. Details of the method can be found in Cosma and Enescu (2001). Main characteristics of these sources are listed in Table 1.

Table 1. Main characteristics of the sources used in the Ketzin pilot study.

Characteristic	VIBSIST	MiniVib	Weight drop
Type	Swept impact, VIBSIST 1000	Vibrator MHV 2.7	Impact EWG III
Contractor	Vibrometric, Helsinki	GGA[1] institut, Hanover	Geophysik GGD[2], Leipzig
Specification	Energy ≈ 2000 kJ up to 1000 J per impact	Baseplate mass: 138 kg Reaction mass: 181 kg Peak force: 27600 N Freq. range: 16-500 Hz	≈ 250 kg Energy ≈ 9.5 kJ
Spectrum	Variable (controllable)	Variable (controllable)	Variable (depend on weight)
Repeatability	Yes	Yes	Yes
Field record	Need "shift and stack"	Need correlation and vertical stack (if multiple records)	Need vertical stack (if multiple records)
Operation	Complex	Fairly complex	Fairly complex
Field equipment	Heavy	Moderate to heavy	Moderate to heavy
Approximate production rate	4 min/shot	5 min/shot	3 min/shot

DATA ACQUISITION

The pilot reflection seismic data were acquired in September, 2004. Two perpendicular lines, running mostly along two agricultural roads near the target area of the planned 3D survey, were acquired (Figure 1). The surface relief along the N-S profile (Line 1) is relatively higher than that of the E-W profile (Line 2). Surface conditions along the two lines varied. Line 1 was a traditional agricultural road, while Line 2 consisted of a hard soil that had been compressed by heavy military equipment.

Although the pilot study consisted of both testing of source and receiver performance, in this paper we focus on the source comparison. The three different sources were tested along the two lines. The measurements were carried out according to the same scheme for every source. On the first day, tests and parameter tuning were done at five selected locations on or close to

[1] Leibniz Institute for Applied Geosciences
[2] Gesellschaft für Geowissenschaftliche Dienste m.b.H.

Line 2. These test points showed that shot records acquired at soft ground conditions had broader bandwidth than those acquired at unconsolidated and hard ground conditions, confirming that ground conditions have an influence on the frequency content of the data. On the following 2-3 days, data were acquired by shooting at all stations (source and receiver spacing of 20 m) on both profiles, allowing CMP stacked sections to be produced. Data were recorded on 240 channels (fixed spread). Sources activated on Line 1 were also recorded on Line 2, and vice versa, providing the possibility for a (pseudo) 3D analysis of the survey area. However, for source comparison purposes the data were processed in a 2D manner. Only a few selected stations were skipped due to the presence of underground gas lines. It should be noted that, regardless of the technical and logistic problems, the lack of several CMPs at the end of Line 1 in the MiniVib data is due to missing shot points because of acquisition time limitations. The tests also included comparison of 10 Hz and 28 Hz single geophones and 10 Hz geophone arrays on Line 2 and a comparison of geophones planted on the surface and in holes 30-40 cm deep. Evaluation of geophone performance and dominant frequency content of the data resulted in using the data recorded by the 28 Hz geophones for this study. A summary of the acquisition parameters is provided in Table 2. On-site data quality control was used to determine the vertical stacking for each source. This control showed that the use of 3, 5 and 5-8 stacks for the VIBSIST, MiniVib and weight drop sources, respectively, appeared to be sufficient for acquiring data with acceptable quality.

Table 2. Acquisition parameters.

Parameter	**Detail**
Sources	Weight drop, VIBSIST and MiniVib
Profile	
Length	2.4 km
Number of stations/line	120 stations
Number of shots/line	113-115 (Weight drop), 107-114 (VIBSIST) and 71-117 (MiniVib)
Shots per station	5-8 (Weight drop), 3 (VIBSIST) and 5 (MiniVib)
Receivers	
Natural geophone frequency	10 Hz and 28 Hz (single), 10 Hz array
Spacing	20 m
Recording	
Recording system	SERCEL 408 system
Record length	3 s (Weight drop), 30 s (VIBSIST) and 18.5 s (MiniVib)
Sweep length	27 s (VIBSIST) and 16 s (MiniVib)
Sampling interval	1 ms

DATA PROCESSING

Examples of typical unprocessed, but stacked, correlated or decoded, shot gathers from the three different sources are shown in Figure 4. To directly compare the data quality recorded by individual sources, the raw shot gathers with and without trace normalization (balancing) are displayed. The strong amplitude distortion at near offset traces (< 500 m) is probably due to the combination of source-generated noise, engine noise and air blasts. In the shot gathers with trace normalization, the direct P-wave, ground roll and source-generated noise are clearly seen, as well as reflections. There is a noticeable decrease in signal-to-noise ratio on some of the far offset traces (> 1300 m).

We have focused our data processing and analysis on the upper 1.5 s since the target horizon for the CO_2SINK project is at about 700 m depth. Several conventional processing steps were applied in order to enhance the data in the upper 1.5 s (Table 3). Given the differing nature of the sources, we decided to process each data set independently of the others when producing stacked sections. In the pre-processing phase, the weight drop data required vertical stacking, the MiniVib data required correlation and the "shift and stack" process was applied to the VIBSIST data. The MiniVib source also required vertical stacking if more than one shot per vibrator point was performed. Testing showed that using 5, 5 and 3 shots for the weight drop, MiniVib and VIBSIST data, respectively, produced data of comparable quality for each source. The measured sweeps (input signal from the MiniVib) were used in the correlation process of the MiniVib data. The VIBSIST records require application of decoder software that performs some preprocessing steps and then the "shift and stack" algorithm on the raw preprocessed data (Cosma and Enescu 2001). The preprocessing steps included: bandpass filtering (10-100 Hz), amplitude adjustment by applying an alpha-trimmed median filter, and delay time corrections by analyzing travel times of source-receiver pairs.

For the VIBSIST data, first arrival times were picked on the decoded shot records and near surface structure was determined. Static corrections were then computed and applied to the data. Deconvolution balanced the spectrum and improved the resolution. Source-generated noise, such as ground roll, is prominent on unfiltered records and contaminated the near offset (0-500 m) traces for all sources. Ground roll (coherent noise) appears within a typical cone, characterized by high-amplitude and low frequency energy which is produced by the near surface geology. Quantitative comparison of source-generated ground roll is difficult, however, qualitative shot to shot variations due to near surface conditions are clearly seen on records from all three sources. Bandpass filtering removed some of the ground roll, but it was still necessary to apply a bottom mute. Based on amplitude spectra, frequency filters of 30-85 Hz were designed to limit the influence of high and low fre-

quency noise. Although linear noise removal (e.g. f-k filtering) is effective and it is often an option for suppressing ground roll, this technique was skipped in order to avoid introducing artifacts into the data. After CMP sorting, careful velocity analysis was performed by picking velocities in constant velocity stacked and/or semblance panels. After NMO, surface consistent residual statics were computed along chosen reflection horizons (T1 and K2 horizons). By applying residual statics before velocity analysis and re-stacking, the stacked sections were improved.

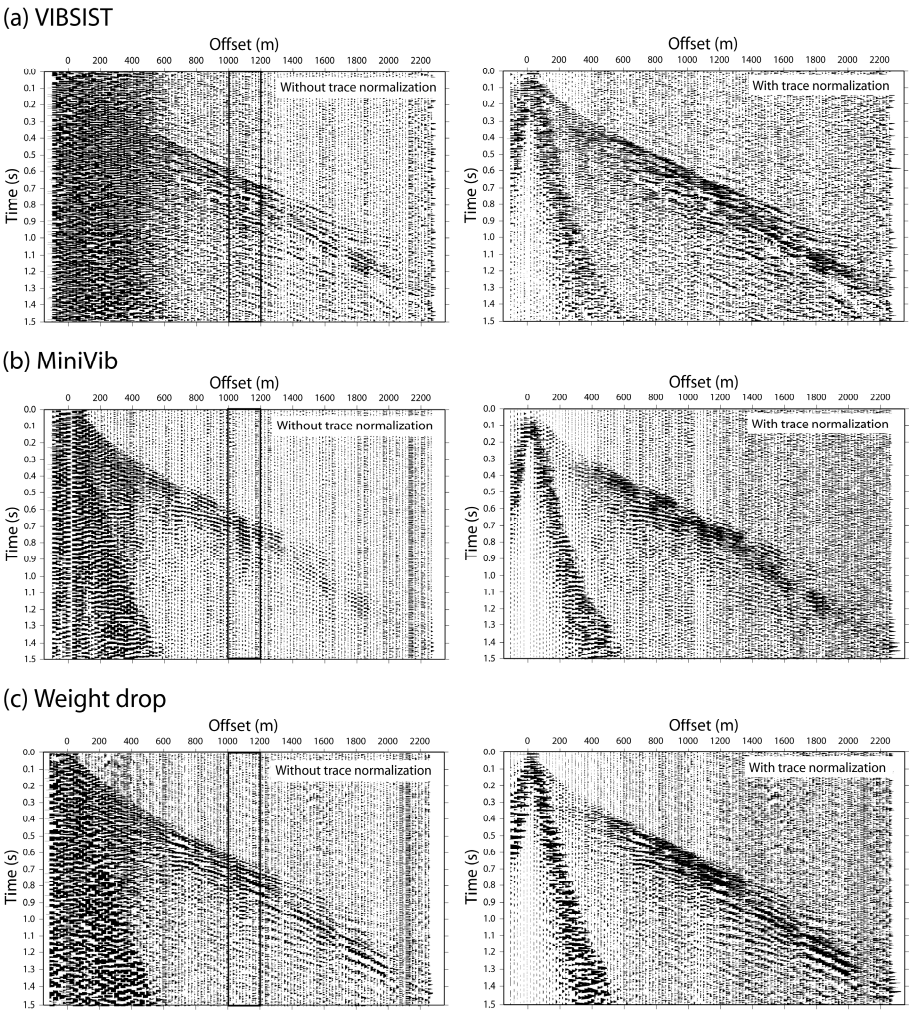

Figure 4. A raw shot gather (left) and average amplitude versus traveltime (right) of (a) VIBSIST, (b) MiniVib and (c) Weight drop. Black windows marked the offset range of amplitude analysis.

Processing flows for the MiniVib and weight drop differed in some aspects from the VIBSIST processing. For the MiniVib data a minimum phase

signal transformation was applied before deconvolution. This transformation was designed to improve the deconvolution result and allows a comparison with the minimum phase signals of the impact sources. The bandpass filters applied in the MiniVib and weight drop processing were 40-100 Hz and 33-110 Hz, respectively. The same velocity function could not be used for NMO prior to stacking for all three sources since the optimum velocity function is dependent upon quality of the statics applied, data bandwidth and signal-to-noise ratios. Therefore, velocity analysis was performed individually for each data set in order to produce the most coherent respective stack, as was the case for the static calculations.

Table 3. Processing flow.

Processing step	**Description**
1. Data import	Correlation (MiniVib data) and/or stack of shot gathers, shift (VIBSIST data).
2. Geometry	Assign input source and receiver locations into header.
3. Trace editing	Kill bad traces and fix polarity reversals.
4. True amplitude recovery	Compensate for geometrical spreading by scaling by t^2.
5. Refraction statics	Model near-surface structure and calculate static corrections.
6. Minimum phase transformation (for MiniVib)	To improve the deconvolution result and to compare with the minimum phase signals of the impact sources.
7. Deconvolution	Minimum phase predictive deconvolution with a design gate limited to the time range of clear reflections. (offset:t1-t2 = 0:0-150/60:40-150/440:275-1135/900:515-1500).
8. Bandpass Filter	15-30-85-135 Hz. (VIBSIST), 30-40-100-150 (MiniVib), 23-33-110-160 (weight drop).
9. AGC	Adjust amplitudes for display using 300 ms window.
10. Top mute / bottom mute	Zero all data amplitude before and including first arrivals / Zero all cone of ground roll.
11. Sort to CDP Domain	Reorder data by common midpoint number.
12. Velocity analysis - Pass 1	Integrate analysis of stacked velocity panels and semblance plots.
13. Residual Statics	Surface-consistent, based on maximum stack power.
14. Velocity analysis - Pass 2	
15. NMO	Apply stacking velocities.
16. Stack	

SIGNAL-TO-NOISE RATIOS

Following Staples *et al*. (1999) and Benjumea and Teixido (2001), a direct comparison of the signal-to-noise ratio can be made using raw data from the three sources. The apparent signal-to-noise ratio, $Q_{S/N}$ is given by:

$$Q_{S/N} = \frac{S_{RMS_{t_0}^{t_0+200ms}}}{N_{RMS_{t_0-200ms}^{t_0}}} \qquad (1)$$

where S_{RMS} is the RMS amplitude measured in a 200 ms window before the first arrival time, N_{RMS} is RMS amplitude measured in a 200 ms window starting from the first arrival time, and t_0 is the first arrival time. This time window was used for analysis since the first arrivals are generally clear with amplitudes significantly higher than the background noise. The apparent signal-to-noise ratio versus offset of the three seismic sources for the offset range 1000-1180 m is shown in Figure 5. This offset range was chosen since the source-generated noise is minimal, but first arrivals are still clear. The analysis was performed on common-offset gathers using stacked traces of five adjacent shots within the selected offset range. The average apparent signal-to-noise ratios of the VIBSIST, MiniVib and weight drop sources within this analyzed offset range are 5.58, 4.70 and 5.30, and their standard deviations are 1.82, 0.98 and 1.74, respectively. These values are consistent with qualitative signal-to-noise ratio estimation by visual inspection of the seismic traces (Figure 4). The signal-to-noise ratio of the VIBSIST and weight drop data is relatively higher than the MiniVib data, but they appear to have a larger deviation than the MiniVib data, implying that the MiniVib source may have the better repeatability. Note that the larger oscillations of the signal-to-noise ratios of the VIBSIST and weight drop data compared to the MiniVib data (Figure 5) may be due to local cultural noise.

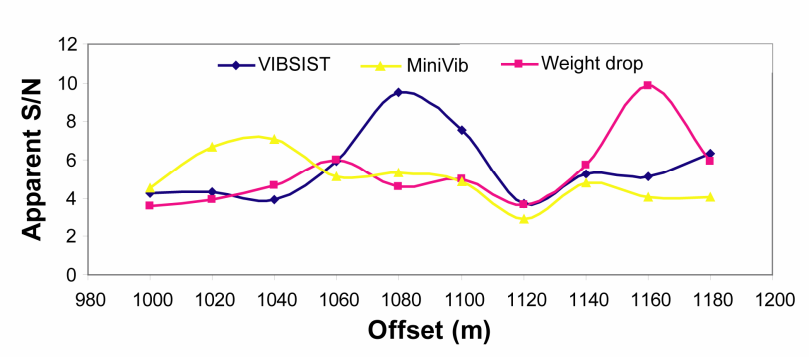

Figure 5. Apparent signal-to-noise ratio of different source at selected offset from Figure 4. Note that 5 adjacent shots were used for this analysis.

SIGNAL PENETRATION AND FREQUENCY CONTENT

Amplitude decay analysis can provide an indication of the source-generated energy and signal penetration depth. A number of studies have been carried out where the amplitude decay with traveltime has been interpreted in terms of signal penetration (e.g. Mayer and Brown 1986; Barnes 1994; Steer *et al*. 1996; Juhojuntti and Juhlin 1998). In these studies, the signal penetration limit is defined as that time where the source-generated energy ceases to decrease temporally and amplitudes are on the same level as the incoherent, time independent background noise. The depth corresponding to this time can be, at least, a relative indication of the maximum depth of effective signal penetration since amplitudes at later traveltimes are almost entirely dominated by ambient noise. Furthermore, only extremely strong reflections, if any, should be seen on the seismic section at later traveltimes. However, continued amplitude decay beyond a given time is no guarantee that significant reflected energy has been recorded because not only reflective energy, but also refractions, surface waves, guided waves, and various forms of backscattered waves contribute to the data amplitudes. Consequently, the decay curve is an indirect indication of the true reflection amplitude decay.

The signal penetration of the VIBSIST, weight drop and MiniVib sources were compared in a quantitative manner by studying the amplitude decay curves. Absolute values of seismic traces in the offset interval 1000-1200 m were used for estimating the amplitude decay. As seen in the raw shot gathers (Figure 4), this offset range was selected for analysis because reflections are not contaminated in the "optimum window" (Hunter *et al*. 1984). To perform this analysis, the absolute amplitudes of the traces from five adjacent shots within this offset range were used. These traces were then stacked by taking the mean values of all traces in this offset range to form a single trace for each shot. In this method, true amplitude is preserved and the relative lateral variations in amplitude are reduced. Stacked traces from five adjacent shots were then averaged to obtain a master trace. Average amplitudes of this trace were then calculated on 100 ms time windows from 0 to 1.5 s. Given that the first arrival is at about 500 ms in this offset range, the amplitude values from the first to the fifth time windows represent background (ambient) noise levels. In order to compare peak amplitudes of the three seismic sources, amplitudes relative to background levels versus traveltime were plotted (Figure 6a). Since amplitudes remain above background levels down to record times of 1.5 s, signal penetration for the three sources appears to be at least to depths corresponding to this time. For explosive sources, Juhojuntti and Juhlin (1998) found that the peak amplitude in the first arrival time window increases with the size of the charge, in agreement with source generated energy increasing with charge size. The MiniVib data show the highest peak amplitude in the first arrival time window, whereas the amplitudes of the VIBSIST data and the weight drop data

are lower, suggesting that the MiniVib is putting the largest amount of energy into the ground. However, if amplitude is normalized to peak amplitude for each source (Figure 6b), the amplitude decay curves differ after the 700 ms time window. Normalized amplitude decreases more slowly for the VIBSIST data, suggesting that this source has the greatest penetration.

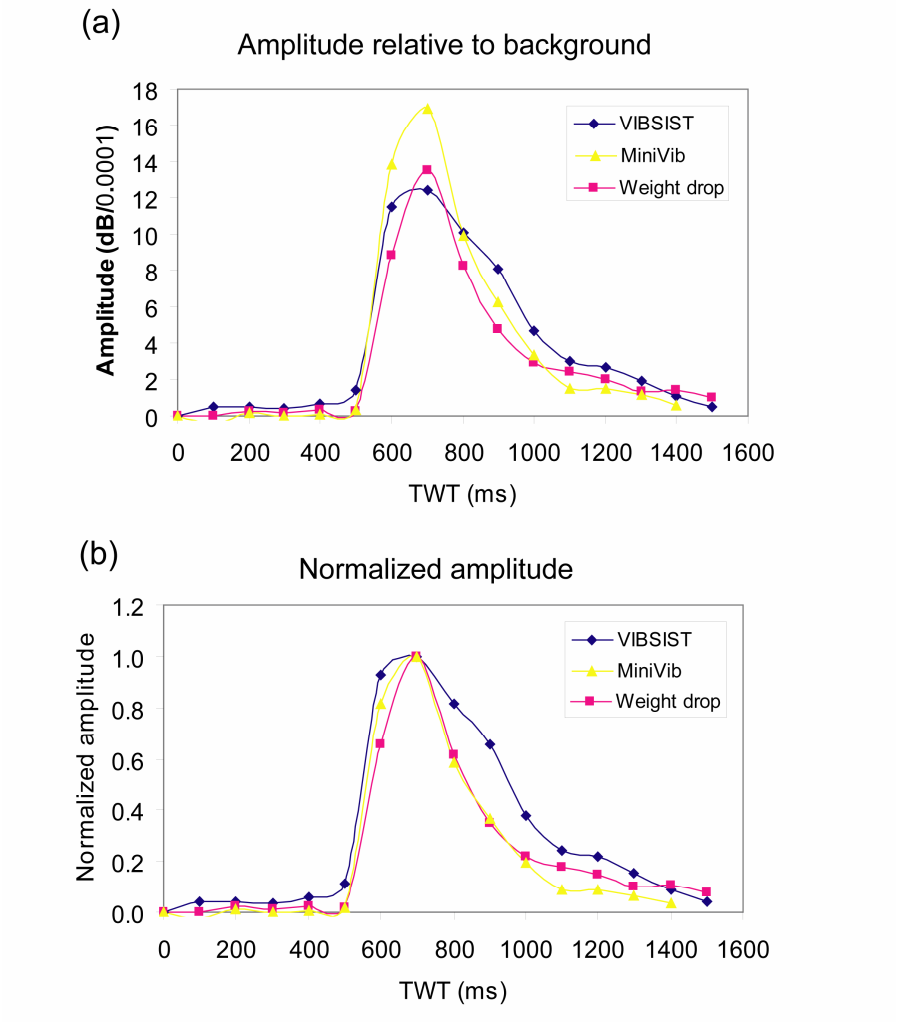

Figure 6. Signal penetration of three seismic sources by comparing (a) amplitude relative to background versus traveltime plot and (b) normalized amplitude versus traveltime plot.

Amplitude spectra for each source in the same offset windows as shown in Figure 4 are shown in Figure 7. All three sources have dominant signal frequencies of around 30-120 Hz (> 2 octaves), providing enough bandwidth for resolving the geological target. Quantitatively, assuming a dominant

frequency at 700 ms TWT of 40 Hz and a velocity of 3000 m/s, the 80 m thick target formation is well resolved. The high frequency portions of the amplitude spectra differ for the three sources. The amplitude spectrum of the MiniVib is controlled by the frequencies put into the ground, 30-150 Hz. Amplitudes outside the 30-150 Hz range for the MiniVib should be regarded as noise. No upper limit exists for the frequencies put into the ground by the VIBSIST source, however, the VIBSIST data were wide-band filtered to improve signal-to-noise ratio before applying the shift and stack process. The falloff in amplitudes at high frequencies reflects this pre-processing step. Weight drop amplitude spectra from time windows prior to the first arrival show a flat spectrum, similar to that shown in Figure 7. This proves that no useful energy is put into the ground by the weight drop at frequencies greater than 150 Hz. Even the low amplitudes in the frequency range 100-150 Hz are indicative that it is mainly noise that is recorded at these frequencies by the weight drop source.

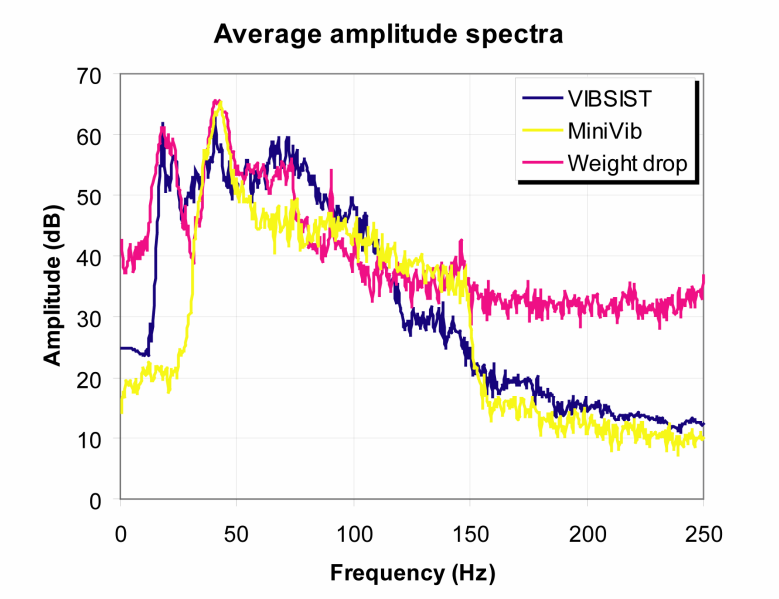

Figure 7. Average amplitude spectra of three seismic sources calculated from traces in offset between 1000-1200 m as shown in Figure 4.

Resolution naturally decreases with depth due to attenuation preferentially removing the higher frequencies in the propagating seismic waves (Knopoff 1964; Praeg 2003). The low frequency end of the spectrum is attenuated primarily by the frequency response of the geophone and field record filtering, while the decrease at the high end of the spectrum is mainly due to propagation through the earth. Therefore, a comparison of relative amplitude decay curves from the three sources in different frequency bands may give an indication of which frequency band gives the best penetration for a given

source (Figure 8). The amplitude decay of the various frequency bands for the VIBSIST data is less rapid than for the other two sources. This observation also suggests that the VIBSIST source has the greatest penetration.

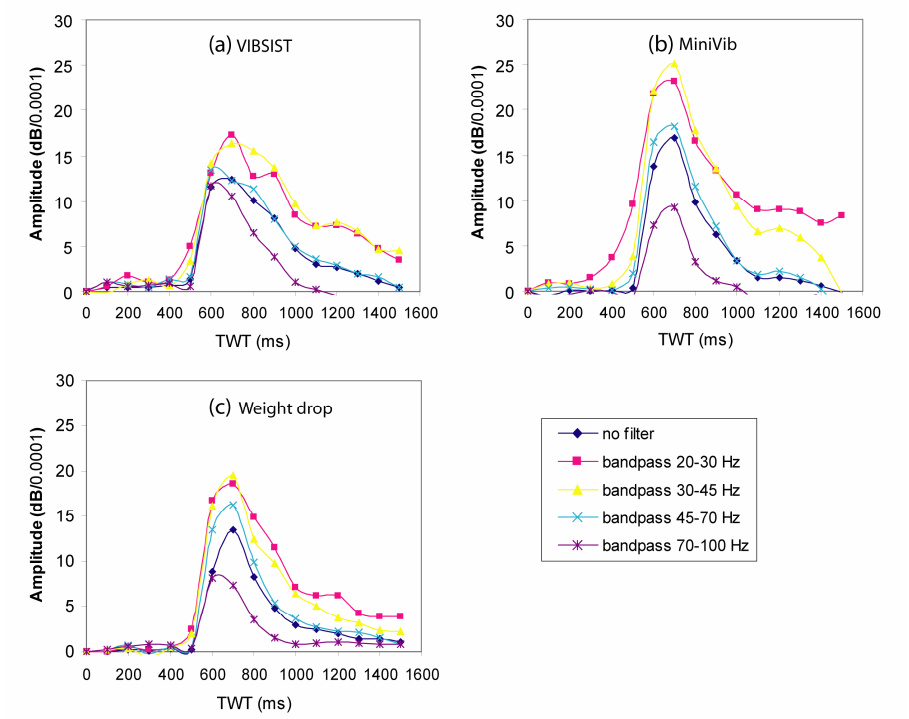

Figure 8. Amplitude relative to background versus travetime of different sources at different frequency bands.

COMPARISON OF SEISMIC SECTIONS

CMP stacks from the three different sources are shown in Figures 9 and 10. Figure 11 depicts blow-ups of the Line 2 stacked sections between CMP 660 and 720 and traveltime of 0.35 s and 0.7 s. The L4, K2 and K3 reflections are marked. SF denotes the position of the Stuttgart Formation. For our comparison we consider the T1, L4, K2, and K3 reflection horizons.

The sections from all three sources (Figure 9 and 10) show the reflections corresponding to the major lithological interfaces in the area. Line 1 is characterized by an overall lower signal-to-noise ratio compared to Line 2. In particular, the northern part of Line 1 up to CMP 1100 is of poor signal quality. In this area, the near-surface consists of a thick Quaternary sand layer (30 m) which significantly attenuates the seismic waves. Whereas the VIBISIST and the weight drop sources show clear reflections below the K2 horizon (0.45 s to 0.5 s, about 450 m to 500 m depth) the MiniVib section (Figure 9b) shows only some discontinuous reflections. The sections from

the two impact sources show the same events down to a weak reflection at 1.3 s to 1.4 s (approx. 1400 m -1500 m depth).

All sections from Line 2 (Figure 10) show clear reflections down to 1.4 s. In Figure 10a the deepest reflector (1.3 s to 1.4 s) is characterized as a nearly continuous event along all CMPs, showing the higher signal energy transmitted by the VIBSIST source. A more detailed signal analysis with respect to the target horizons is shown in Figure 11. In this time window (0.35 s to 0.7 s) the reflection signals of the MiniVib data (Figure 11b) show higher frequencies (higher resolution) than the signals of the VIBSIST data (Figure 11a) and of the weight drop source (Figure 11c). The transmitted signal energy of the three sources is high enough to image the reflections from the L4 to K2 reflectors at all CMPs. Below the K2 reflection the MiniVib data show less continuity (e.g. K3 reflector, CMP 660 to 685) than the two impact sources.

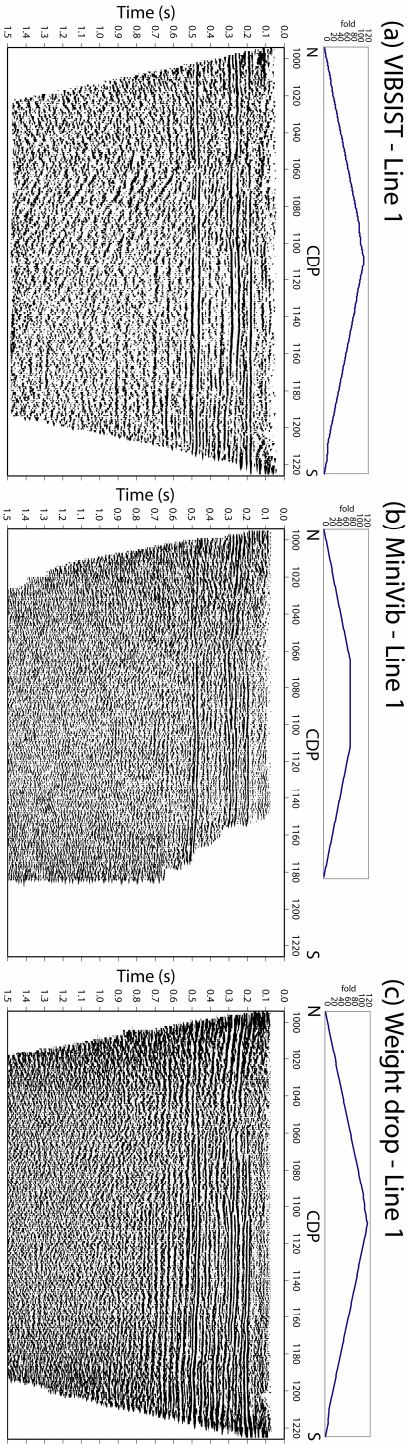

Figure 9. Stacked section and fold plot of Line 1. (a) VIBSIST section, (b) MiniVib section and (c) Weight drop section.

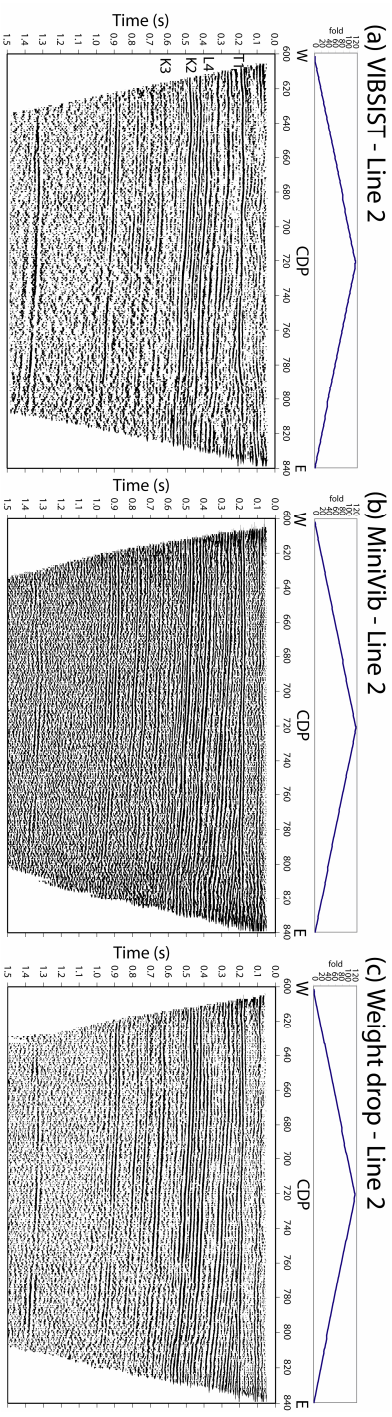

Figure 10. Stacked section and fold plot of Line 2. (a) VIBSIST section, (b) MiniVib section and (c) Weight drop section. T1= near base Tertiary, L4 = top Triassic (assumed), K2 = top Weser Formation, K3 = near top of Grabfeld Formation.

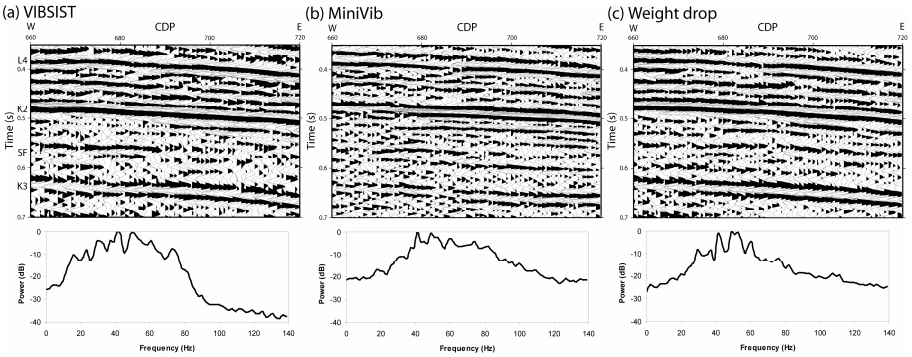

Figure 11. Blow-ups of the Line 2 stacked sections from (a) VIBSIST (b) MiniVib and (c) Weight drop sources. L4 = top Triassic (assumed), K2 = top Weser Formation, SF = Stuttgart Formation, K3 = near top of Grabfeld Formation. Bottom panels show the amplitude spectrum of each section.

DISCUSSION AND CONCLUSIONS

We have characterized three seismic surface sources with respect to their signal-to-noise-ratio, signal penetration and frequency content by analysis of raw shot gathers and stacked sections along two lines in the vicinity of the 3D seismic area at the Ketzin site. In comparison to explosive sources there are some particularities of the surface sources which have to be taken into account. Compacting effects at the source point have a strong influence on the data quality. The stability of the source signal waveform is of critical importance with respect to the improvement of the signal-to-noise ratio by vertical stacking of pulse sequences at each source point. One of the main shortcomings of surface sources is the presence of strong noise waves (e.g. surface and air-coupled waves). Near surface conditions strongly influence the signal bandwidth (resolution) and signal energy. At the Ketzin site, the high variability of the near surface conditions is expressed by the difference in reflectivity of the two CMP lines (Figure 9 and 10). All these factors need to be taken into account for surface seismic source selection.

The three sources image the upper 500 ms with approximately the same clarity. The MiniVib data show the highest resolution (Figure 11) for this part of the time section, but the signal reflection energy below about 500 ms is lower than that of the two impact sources. The lack of deeper reflectivity in certain portions of the lines may be due to the seismic sources generating insufficient energy, but also to the lack of lower frequency energy in the spectrum. The VIBSIST source gives a better image below 900 ms than the weight drop source and the MiniVib. This is in agreement with the analysis of raw shot gathers, where clear evidence is found for a higher signal-to-noise ratio of the seismic signals and greater signal penetration for the VIBSIST source compared to the other tested sources. This is indicated by the

high apparent signal-to-noise ratio in the offset range of 1000 m to 1180 m and the slowly decreasing normalized amplitude beyond 700 ms traveltime in Figure 6b. There is an overall tendency that the content of higher frequency signals decreases with increasing source power, consistent with other field observations (Herbst *et al*. 1998).

The Ketzin pilot study shows that the VIBSIST, weight drop and MiniVib are suitable sources for high resolution seismic surveys down to a depth of about 1 km. The average amplitude spectra show that all three sources provide enough bandwidth for resolving the geological target (e.g. the Weser and Stuttgart Formations). The CMP sections of the MiniVib source show the highest frequency signals to about 500 ms (approx. 500 m depth), but the shallowest signal penetration. The VIBSIST source generates signals with the highest signal-to-noise ratio and the greatest signal penetration of the tested sources. In particular, the reflections below 900 ms (approx. 1 km depth) are best imaged by the VIBSIST source. In terms of signal-to-noise ratio and signal penetration, the weight drop performance falls in between these two sources. Apart from the source-generated noise, present on near offset traces for all three sources, ambient noise is higher at far offsets on both the MiniVib and weight drop data. At the cost of increased acquisition time, this noise could possibly be reduced by increased vertical stacking. Since all 3 sources imaged the target horizon, the choice of source for the 3D survey (Juhlin *et al*. 2007) was based mainly on logistics and cost. Given that time was an important factor, the weight drop source was recommended as the primary source for the 3D survey. For monitoring purposes within the project framework, 2D data were acquired using the VIBSIST source (Juhlin *et al*. 2007).

ACKNOWLEDGEMENTS

The authors gratefully acknowledge M. Stiller (Section 2.2, GFZ Potsdam) for support in preparation and conduction of the field work. We wish to thank the Geophysik-GGD (Leipzig), GGA-institute (Hanover) and Vibrometric Oy (Helsinki) source crews for good cooperation in the field. We also thank A. Sippel and J. Mlynek for their support while conducting the experiment. We acknowledge the Geophysical Instrument Pool Potsdam (GIPP) for its technical support. The European Commission is gratefully acknowledged for their funding of the "CO_2SINK - CO_2 Storage by Injection into a Natural Storage at Ketzin", Project No. 502599. Stefan Lueth is thanked for his technical information of the sources. Comments from Mustafa Al-Ali, Lorenzo Petronio, Giuliana Rossi and the editor helped to improve the paper.

REFERENCES

Arts R., Eiken O., Chadwick A., Zweigel P., van der Meer L. and Zinszner B. 2004. Monitoring of CO_2 injected at Sleipner using time-lapse seismic data. *Energy* **29**, 1383-1392.

Barbier M.G., Bondon P., Mellinger R. and Viallix J.R. 1976. MiniSOSIE for shallow land seismology. *Geophysical Prospecting* **24**, 518-527.

Barnes A.E. 1994. Moho reflectivity and seismic signal penetration. *Tectonophysics* **232**, 299-307.

Benjumea B. and Teixido T. 2001. Seismic reflection constraints on the glacial dynamics of Johnsons Glacier, Antarctica. *Journal of Applied Geophysics* **46**, 31-44.

Buhnemann J. and Holliger K. 1998. Comparison of high-frequency seismic sources at the Grimsel test site, central Alps, Switzerland. *Geophysics* **63**, 1363-1370.

Cosma C. and Enescu N. 2001. Characterization of fractured rock in the vicinity of tunnels by the swept impact seismic technique. *International Journal of Rock Mechanics and Mining Sciences* **38**, 815-821.

Davis T.L., Terrell M.J., Benson R.D. and Kendall R.R. 2002. Seismic Monitoring of the CO_2 Flood at Weyburn Field, Saskatchewan, Canada. EAGE 64th Conference & Exhibition, Florence Italy.

Feroci M., Orlando L., Balia R., Bosman C., Cardarelli E., and Deidda G. 2000. Some considerations on shallow seismic reflection surveys. *Journal of Applied Geophysics* **45**, 127-139.

Förster A., Norden B., Zinck-Jørgensen K., Frykman P., Kulenkampff J., Spangenberg E., Erzinger J., Zimmer M., Kopp J., Borm G., Juhlin C., Cosma C. and Hurter S. 2006. Baseline characterization of the CO_2SINK geological storage site at Ketzin, Germany. *Environmental Geosciences* **13**, 145-161.

Herbst R., Kapp I., Krummel H. and Luck E. 1998. Seismic sources for shallow investigations: A field comparison from Northern Germany. *Journal of Applied Geophysics* **38**, 301-317.

Hunter J.A., Pullan S.E., Burns R.A., Gagne R.M. and Good R.L. 1984. Shallow seismic reflection mapping of the overburden-bedrock interface with the engineering seismograph—Some simple techniques. *Geophysics* **49**, 1381-1385.

Juhojuntti N. and Juhlin C. 1998. Seismic lower crustal reflectivity and signal penetration in the Siljan Ring area, Central Sweden. *Tectonophysics* **288**, 17-30.

Juhlin C., Giese R., Zinck-J¸rgensen K., Cosma C., Kazemeini H., Juhojuntti N., Lüth S., Norden B., and. Förster A. 2007. 3D baseline seismics at Ketzin, Germany: The CO2SINK project. *Geophysics* **72**, B121-B132.

Jongerius P. and Helbig K. 1988. On-shore high-resolution seismic profiling applied to sedimentology. *Geophysics* **53**, 1276-1283.

Knapp R.W. and Steeples D.W. 1986. High-resolution common depth-point reflection profiling: Field acquisition parameter design. *Geophysics* **51**, 283–294.

Knopoff L. 1964. Q. *Reviews of Geophysics* **2**, 625-660.

Mayer J.R. and Brown L.D. 1986. Signal penetration in the COCORP Basin and Range-Colorado plateau survey. *Geophysics* **51**, 1050–1055.

Metz B., Davidson O., de Coninck H., Loos M. and Meyer L. 2005. Carbon Dioxide Capture and Storage: IPCC Special Report, Cambridge University Press, UK and New York.

Park C.B., Miller R.D., Steeples D.W. and Black R.A. 1996. Swept impact seismic technique (SIST). *Geophysics* **61**, 1789-1803.

Praeg D. 2003. Seismic imaging of mid-Pleistocene tunnel-valleys in the North Sea Basin—high resolution from low frequencies. *Journal of Applied Geophysics* **53**, 273-298.

Pullan S.E. and MacAulay H.A. 1987. An in-hole shotgun source for engineering seismic surveys. *Geophysics* **52**, 985-996.

Reinhardt H.G. 1993. Regionales Kartenwerk der Reflexionsseismik. VEB Geophysik Leipzig.

Sheriff R.E. 1975, Factors Affecting Seismic Amplitudes. *Geophysical Prospecting* **23**, 125-138.

Staples R.K., Hobbs R.W. and White R.S. 1999. A comparison between airguns and explosives as wide-angle seismic sources. *Geophysical Prospecting* **47**, 313-339.

Steeples D.W. and Miller R.D. 1990. Seismic reflection methods applied to engineering, environmental, and groundwater problems. In: *Geotechnical and environmental geophysics, I: Review and tutorial,* Vol. 1 (Ward, S. H., Ed.), pp. 1-30, Soc. Explor. Geophys.

Steer D.N., Brown L.D., Knapp J.H. and Baird D.J. 1996. Comparison of explosive and vibroseis source energy penetration during COCORP deep seismic reflection profiling in the Williston Basin. *Geophysics* **61**, 211-221.

Telford W.M., Geldart L.P. and Sheriff R.E. 1990. *Applied Geophysics*. Cambridge University press, 770 pps.

Woodward D. 1994. Contributions to a shallow aquifer study by reprocessed seismic sections from petroleum exploration surveys, eastern Abu Dhabi, United Arab Emirates. *Journal of Applied Geophysics* **31**, 271-289.

Wright C., Wright J.A. and Hall, J. 1994. Seismic reflection techniques for base metal exploration in eastern Canada: examples from Buchans, Newfoundland. *Journal of Applied Geophysics* **32**, 105-116.

Ziqiu X. and Takashi O. 2004. Time-lapse crosswell seismic tomography and well logging to monitor the injected CO_2 in an onshore aquifer, Nagaoka, Japan. IEA Monitoring and Verification Workshop, Santa Cruz.